ELSEVIER

Catalysis Today 66 (2001) 411–417

CATALYSIS TODAY

www.elsevier.com/locate/cattod

Modeling of the enantioselective hydrogenation of 1-phenyl-1,2-propanedione over Pt/Al_2O_3 catalyst

Esa Toukoniitty*, Päivi Mäki-Arvela, Johan Wärnå, Tapio Salmi

Laboratory of Industrial Chemistry, Process Chemistry Group, Åbo Akademi, FIN-20500 Turku/Åbo, Finland

Abstract

A kinetic model was developed for the enantioselective hydrogenation of 1-phenyl-1,2-propanedione based on parallel racemic and enantioselective routes in the presence of cinchonidine. The Langmuir–Hinshelwood type of competitive adsorption approach was used in the model, which was combined with a batch reactor model. The proposed model could sufficiently describe the observed kinetic results. © 2001 Elsevier Science B.V. All rights reserved.

Keywords: Enantioselective hydrogenation; 1-Phenyl-1,2-propanedione; Pt/Al_2O_3 catalyst

1. Introduction

Enantioselective hydrogenation of α-ketoesters over cinchonidine-modified Pt catalysts has been intensively investigated and both Langmuir–Hinshelwood [1,2] and Eley–Rideal type [3] kinetic models have been proposed for this reaction. The major obstacle in the discrimination of rival kinetic models is the lack of precise information about the interaction between the modifier, the substrate and the catalyst surface. The mechanism suggested by Margitfalvi et al. [3] has been excluded due to the saturation of enantiomeric excess (ee) at very low cinchonidine (**CD**) concentrations and the ee should be according to the model independent of time [4]. The models found in literature considering the enantioselective hydrogenation of α-ketoesters involved different types of basic assumptions concerning the active sites, where the enantiodifferentiation takes place. Blaser et al. [1] has considered only one kind of active sites, where hydrogen, ethyl pyruvate and **CD** can competitively adsorb. An alternative approach to modeling of the enantioselective hydrogenation of α-ketoesters is the two-site, two-step mechanism, according to which both modified and non-modified sites are considered.

1-Phenyl-1,2-propanedione (**A**), Fig. 1, is a suitable molecule to investigate the enantioselective hydrogenation of conjugated carbonyl bonds [5,6]. It contains a phenyl ring and two carbonyl groups. Under reaction conditions, in the presence of **CD** the most important product is (*R*)-1-hydroxy-1-phenylpropanone (**B**), which is an important intermediate in the synthesis of drugs [7,8]. In the absence of **CD** phenyl ring is hydrogenated, too. The reaction scheme is displayed in Fig. 2. Some other groups have also investigated the enantioselective hydrogenation of diones [9–12]. The kinetic aspects in the enantioselective hydrogenation of diones has been considered in the previous studies, but there do not exist complete kinetic models for these reactions combined to the reactor model.

The aim of the current work was to describe shortly the qualitative kinetic aspects and to develop a kinetic model for enantioselective hydrogenation of **A**. The parameters in the kinetic experiments were the initial

---

* Corresponding author. Tel.: +358-2-215-4479;
fax: +358-2-215-3248.
E-mail address: etoukoni@abo.fi (E. Toukoniitty).

PII: S0920-5861(00)00638-6

Nomenclature

c	concentration
D	adsorption term
E_A	activation energy
k	rate constant
K	equilibrium constant
m_{cat}	mass of catalyst
Q	residual sum of squares, objective function
r	rate
R	gas constant, 8.3145 $J\,K^{-1}\,mol^{-1}$
t	time
T	temperature
V_L	liquid phase volume
ν	stoichiometric co-efficient

Subscripts and superscripts

cat	catalyst
i	component, general index
j	reaction step
L	liquid
$*$	adsorption site

concentration of the reactant, the temperature and the effect of **CD**.

2. Experimental

Hydrogenation experiments were carried out in a pressurized autoclave (Sotelem, Microautoclave System, $V_L = 50\,cm^3$) operating at 5 bar and at 0–25°C. The catalyst, Pt/Al_2O_3 (5 wt.% Pt, Strem, specific surface area $95\,m^2\,g_{cat}^{-1}$, dispersion 40%, mean metal particle size 8.3 nm determined by X-ray diffraction), was activated prior to the reaction under hydrogen flow (hydrogen 99.999%, AGA) for 2 h at 400°C. After cooling the catalyst, the reaction was commenced by injection the modifier, (−)-cinchonidine (96%, Aldrich), the reactant, **A** (99%, Aldrich) and the solvent, ethyl acetate into the reactor. The chemicals were used as received. The modifier concentration in all experiments was $0.0007\,mol\,dm^{-3}$. The stirring rate was 1600 rpm. The concentration of **A** was 0.01, 0.05 or 0.1 $mol\,dm^{-3}$. The mass ratio of **A**-to-platinum was 50. Samples (200 μl) were withdrawn and analyzed with a gas chromatograph equipped with a capillary column (β-Dex 225) and FI-detector. The details of the analytical procedure are described in a previous paper of our group [5].

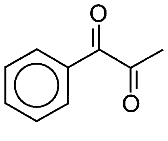

Fig. 1. 1-Phenyl-1,2-propanedione.

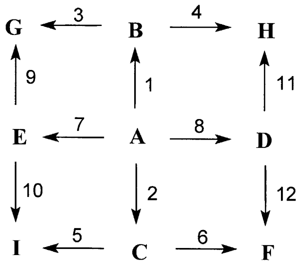

Fig. 2. A complete reaction scheme. **A**: 1-Phenyl-1,2-propanedione, **B**: (*R*)-1-hydroxy-1-phenylpropanone, **C**: (*S*)-1-hydroxy-1-phenylpropanone, **D**: (*S*)-2-hydroxy-1-phenylpropanone, **E**: (*R*)-2-hydroxy-1-phenylpropanone, **F**: (1*S*,2*S*)-1-phenyl-1,2-propanediol, **G**: (1*R*,2*R*)-1-phenyl-1,2-propanediol, **H**: (1*R*,2*S*)-1-phenyl-1,2-propanediol, **I**: (1*S*,2*R*)-1-phenyl-1,2-propanediol.

3. Results and discussion

3.1. Qualitative kinetics

In the presence of modifier, **CD**, in the hydrogenation of **A**, the regioselectivity between 1-hydroxy-1-phenylpropanone (**B**, **C**) and 2-hydroxy-1-phenylpropanone (**D**, **E**) was about 12 (Fig. 3). This is probably due to the higher sterical hindrance of a methyl group at the C_2 position compared to the sterical hindrance of the phenyl ring. The reaction proceeded further to diols (**F**, **G**, **H**, **I**) and the main product among the diols was **H**. The reaction was relatively consecutive, i.e. the hydrogenation of the intermediate hydroxyketones occurred after nearly complete removal of dione. The reason is the stronger adsorption of dione on the Pt surface compared to that of hydroxyketone. The ee of **B**, defined as $ee = |[\mathbf{B}] - [\mathbf{C}]|/([\mathbf{B}] + [\mathbf{C}])$, was about 60% in the

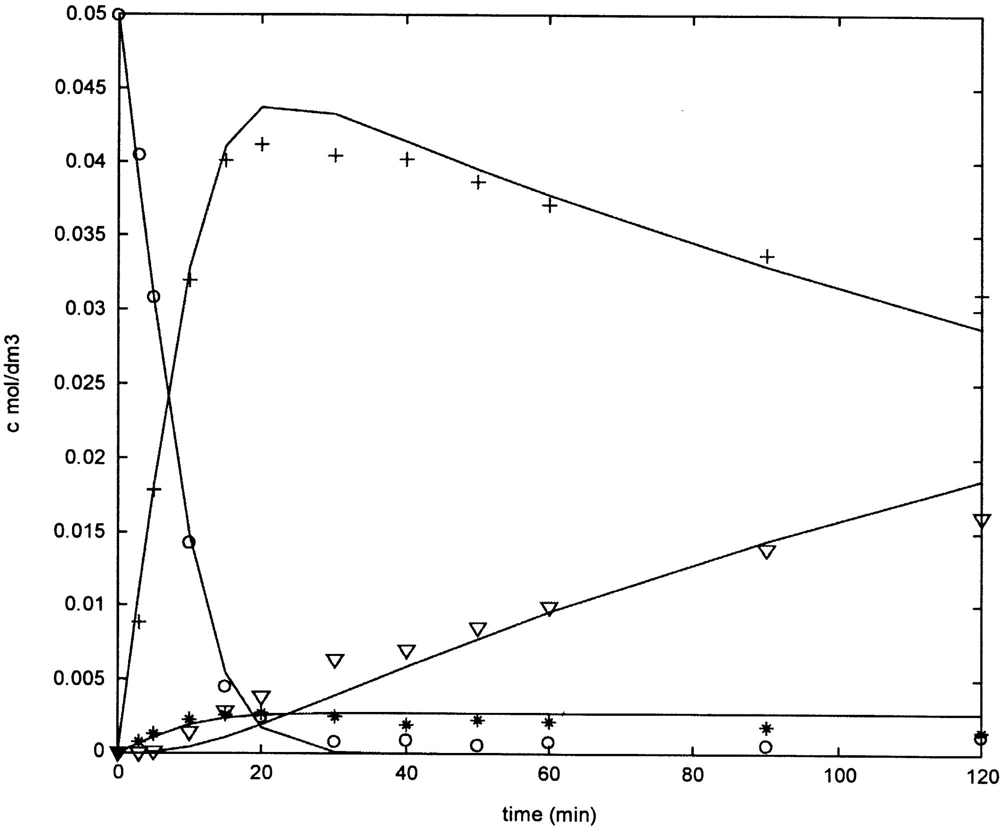

Fig. 3. Typical enantioselective hydrogenation kinetics **A**. Conditions: 25°C, 5 bar hydrogen, solvent ethyl acetate, initial reactant concentration 0.05 mol dm^{-3}. Symbols: (○) 1-phenyl-1,2-propanedione, (+) 1-hydroxy-1-phenylpropanone, (∗) 2-hydroxy-1-phenylpropanone, (▽) diols. The solid lines represent the model fitting.

beginning of the reaction and increased quite linearly with increasing reaction time. At the very end of the reaction the ee of **B** increased to 100% due to the kinetic resolution, i.e. **C** reacted faster to diols than **B**. Analogous results have been observed by Slipszenko et al. [11]. In the racemic hydrogenation of **A**, a rate enhancement was observed compared to the enantioselective hydrogenation due to the unselective hydrogenation of phenyl ring, i.e. cyclohexyl products were confirmed by GC–MS. The initial rates in the racemic and enantioselective hydrogenation of **A** were 19.6 and 8.4 mmol min^{-1} g$_{\mathrm{cat}}^{-1}$, respectively. The presence of **CD** enhanced the hydrogenation rate of butane-2,3-dione and hexane-3,4-dione [11,12], but the difference compared to our system is the lack of phenyl ring. Higher initial concentration of **A** increased the hydrogenation rates, but the ee of **B** remained virtually constant. The highest hydrogenation rates were obtained at 25°C. The effect of temperature on the ee of **B** was very minor. At studied temperatures (0–25°C) the ee of **B** as a function of **A** conversion did not show any variation with temperature. The apparent activation energy evaluated based on the initial hydrogen uptake rate was 23 kJ mol^{-1}.

3.2. Reaction mechanism and rate equations

The kinetic model of **A** hydrogenation is based on the complete reaction scheme presented in Fig. 2. The racemic hydrogenation in the absence of **CD** has a different reaction mechanism as the enantioselective hydrogenation of **A** (see above), therefore the unselective reaction route in the presence of **CD** could not be ignored. The general principle of the kinetic model

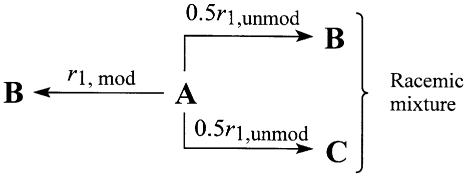

Fig. 4. A model for formation of (*R*)- and (*S*)-1-hydroxy-1-phenylpropanone.

is illustrated in Fig. 4, where both selective and unselective reaction routes are considered. The model consists of following elementary steps, Eqs. (1)–(6):

$$H_2 + 2^{*'} \leftrightharpoons 2H^{*'} \tag{1}$$

$$A_i + ^{*} \leftrightharpoons A_i^{*} \tag{2}$$

$$M + ^{*} \leftrightharpoons M^{*} \tag{3}$$

$$A_i + M^{*} \leftrightharpoons A_iM^{*} \tag{4}$$

$$A_i^{*} + 2H^{*'} \rightarrow A_iH_2 + 2^{*'} + ^{*} \tag{5}$$

$$A_iM^{*} + 2H^{*'} \rightarrow A_iH_2' + 2^{*'} + M^{*} \tag{6}$$

where A_i = **A**, **B**, **C**, **D** or **E**, A_iH_2' = **B**, **C**, **D**, **E**, **F**, **G**, **H** or **I** and A_iH_2' = **B**, **G**, **E** or **I,** where the latter part of products is formed via selective hydrogenation. The reversible substrate and modifier adsorption is assumed to be rapid, whereas the irreversible addition of dissociated hydrogen is rate determining. Both modified and unmodified hydrogenation is considered simultaneously; in step (4) the substrate A_i adsorbs on the modified site and the formed surface complex reacts further with hydrogen to the (*R*)-enantiomer, in step (6) and desorbs from the surface. The reaction rates for each steps can be written as

$$r_1 = r_{1,\mathrm{mod}} + 0.5r_{1,\mathrm{unmod}} \tag{7}$$

$$r_2 = 0.5r_{1,\mathrm{unmod}} \tag{8}$$

$$r_3 = r_{3,\mathrm{mod}} + 0.5r_{3,\mathrm{unmod}} \tag{9}$$

$$r_4 = 0.5r_{3,\mathrm{unmod}} \tag{10}$$

$$r_5 = r_{5,\mathrm{mod}} + 0.5r_{5,\mathrm{unmod}} \tag{11}$$

$$r_6 = 0.5r_{5,\mathrm{unmod}} \tag{12}$$

$$r_7 = r_{7,\mathrm{mod}} + 0.5r_{7,\mathrm{unmod}} \tag{13}$$

$$r_8 = 0.5r_{7,\mathrm{unmod}} \tag{14}$$

$$r_9 = r_{9,\mathrm{mod}} + 0.5r_{9,\mathrm{unmod}} \tag{15}$$

$$r_{10} = 0.5r_{9,\mathrm{unmod}} \tag{16}$$

$$r_{11} = r_{11,\mathrm{mod}} + 0.5r_{11,\mathrm{unmod}} \tag{17}$$

$$r_{12} = 0.5r_{11,\mathrm{unmod}} \tag{18}$$

The surface concentration of hydrogen can be expressed with the adsorption–desorption quasi-equilibria

$$K_H = \frac{c_{H^{*'}}^2}{c_{H_2} c_{*'}^2} \tag{19}$$

The concentration of adsorbed hydrogen from the site balance

$$c_{H^{*'}} + c_{*'} = c_{0^{*'}} \tag{20}$$

where $c_{0^{*'}}$ is the total number of accessible sites for hydrogen adsorption. Thus, $c_{H^{*'}}$ becomes

$$c_{H^{*'}} = \frac{\sqrt{K_H c_{H_2}}\, c_{0^{*'}}}{1 + \sqrt{K_H c_{H_2}}} \tag{21}$$

The quasi-equilibrium adsorption–desorption equilibrium for an organic molecule is expressed as

$$K_{A_i} = \frac{c_{A_i^{*}}}{c_{A_i} c_{*}} \tag{22}$$

Analogously, for the modifier we can write

$$K_M = \frac{c_{M^{*}}}{c_M c_{*}} \tag{23}$$

From the total site balance of organic adsorbates

$$\sum c_{A_i^{*}} + \sum c_{A_iM^{*}} + c_{M^{*}} + c_{*} = c_{00} \tag{24}$$

where c_{00} denotes the total concentration of accessible sites, the concentration of vacant sites is solved

$$c_{*} = \frac{c_{00}}{1 + K_M c_M + \sum K_{A_i} c_{A_i} + \sum K_{A_iM} K_M c_{A_i} c_M} \tag{25}$$

The surface complex A_iM^{*} is described with the expression

$$K_{A_iM} = \frac{c_{A_iM^{*}}}{c_{M^{*}} c_{A_i}} \tag{26}$$

which combined with Eq. (23) gives the concentration $c_{A_iM^{*}}$

$$c_{A_iM^{*}} = K_{A_iM} K_M c_{A_i} c_M c_{*} \tag{27}$$

By inserting the adsorption constants for each compound in Eq. (24) we get the surface complex concentration

$$c_{\mathrm{A}_i\mathrm{M}^*}=\frac{K_{\mathrm{A}_i\mathrm{M}}K_{\mathrm{M}}c_{\mathrm{A}_i}c_{\mathrm{M}}c_{00}}{1+K_{\mathrm{M}}c_{\mathrm{M}}+\sum K_{\mathrm{A}_i}c_{\mathrm{A}_i}+\sum K_{\mathrm{A}_i\mathrm{M}}K_{\mathrm{M}}c_{\mathrm{A}_i}c_{\mathrm{M}}} \tag{28}$$

Now we can write the total rate, r_{Btot} for formation of the main product **B**:

$$\begin{aligned}r_{\mathrm{Btot}}&=r_{1,\mathrm{mod}}+0.5r_{1,\mathrm{unmod}}\\&=k_{1,\mathrm{mod}}c_{\mathrm{H}^*}^2c_{\mathrm{AM}^*}+k_{1,\mathrm{unmod}}c_{\mathrm{H}^*}^2c_{\mathrm{A}^*}\end{aligned} \tag{29}$$

This equation gets its final form after inserting the surface concentrations of hydrogen (Eq. (21)), the organic species C_{A^*} (Eq. (22)) and the surface complex, c_{AM^*} (Eq. (28))

$$\begin{aligned}r_{\mathrm{Btot}}&=k_{1,\mathrm{mod}}\left(\frac{\sqrt{K_{\mathrm{H}}c_{\mathrm{H}_2}}}{1+\sqrt{K_{\mathrm{H}}c_{\mathrm{H}_2}}}\right)^2\frac{K_{\mathrm{AM}}K_{\mathrm{M}}c_{\mathrm{A}}c_{\mathrm{M}}}{D}\\&\quad+k_{1,\mathrm{unmod}}\left(\frac{\sqrt{K_{\mathrm{H}}c_{\mathrm{H}_2}}}{1+\sqrt{K_{\mathrm{H}}c_{\mathrm{H}_2}}}\right)^2\frac{K_{\mathrm{A}}c_{\mathrm{A}}}{D}\end{aligned} \tag{30}$$

where D is an adsorption term

$$\begin{aligned}D&=1+K_{\mathrm{M}}c_{\mathrm{M}}+\sum K_{\mathrm{A}_i}c_{\mathrm{A}_i}\\&\quad+\sum K_{\mathrm{A}_i\mathrm{M}}K_{\mathrm{M}}c_{\mathrm{A}_i}c_{\mathrm{M}}\end{aligned} \tag{31}$$

Because of the consecutive reaction kinetics (see above), only the adsorption of **A** and **M** are considered in adsorption term D', i.e. $D'=1+K_{\mathrm{M}}c_{\mathrm{M}}+K_{\mathrm{A}}c_{\mathrm{A}}+K_{\mathrm{AM}}K_{\mathrm{M}}c_{\mathrm{A}}c_{\mathrm{M}}$. The adsorption constants of other compounds than **A** and **M** were neglected. Generally all the modified reaction steps can be written as

$$r_j=r_{j,\mathrm{mod}}+0.5r_{j,\mathrm{unmod}} \tag{32}$$

$$\begin{aligned}r_{j,\mathrm{mod}}&=k_{j,\mathrm{mod}}\left(\frac{\sqrt{K_{\mathrm{H}}c_{\mathrm{H}_2}}}{1+\sqrt{K_{\mathrm{H}}c_{\mathrm{H}_2}}}\right)^2\\&\quad\times\left(\frac{K_{\mathrm{A}_i\mathrm{M}}K_{\mathrm{M}}c_{\mathrm{A}_i}c_{\mathrm{M}}}{D'}\right)\end{aligned} \tag{33}$$

$$\begin{aligned}r_{j,\mathrm{unmod}}&=k_{j,\mathrm{unmod}}\left(\frac{\sqrt{K_{\mathrm{H}}c_{\mathrm{H}_2}}}{1+\sqrt{K_{\mathrm{H}}c_{\mathrm{H}_2}}}\right)^2\\&\quad\times\left(\frac{K_{\mathrm{A}_i}c_{\mathrm{A}_i}}{D'}\right)\end{aligned} \tag{34}$$

In the unmodified reaction steps $r_{j,\mathrm{mod}}$ term is excluded.

3.3. Reactor model

For parameter estimation purposes, a model for the hydrogenation reactor is necessary. Because of the slow reaction rates at the low temperature and vigorous stirring of the liquid phase, the mass transfer resistances of hydrogen and the organic compounds were ignored. The hydrogen mass balance was also considered by using the hydrogen solubility values found from literature [13] as initial concentrations for hydrogen. For the liquid phase the liquid volume decreased because of sampling and the changes in the liquid volume-to-catalyst ratio were taken into account in calculating the reaction rates. The mass balance of an organic compound becomes

$$\frac{\mathrm{d}c_i}{\mathrm{d}t}=\frac{m_{\mathrm{cat}}}{V_{\mathrm{L}}}\sum \nu_{ij}r_j \tag{35}$$

where ν_{ij} is the stoichiometric coefficient of compound i; m_{cat} and V_{L} denote the mass of catalyst and the liquid volume, respectively. The temperature dependence of the rate constants were described by the law of Arrhenius using the mean temperature 286 K:

$$\ln\frac{k_{\mathrm{T}}}{k_{\mathrm{mean}}}=-\frac{E_{\mathrm{A}}}{R}\left(\frac{1}{T}-\frac{1}{T_{\mathrm{mean}}}\right) \tag{36}$$

The following objective function was minimized during the parameter estimation:

$$Q=\sum_i\sum_t(c_{i,t}-\hat{c}_{i,t})^2 \tag{37}$$

where $c_{i,t}$ is the experimentally recorded concentration of compound i at the reaction time t and $\hat{c}_{i,t}$ is the corresponding concentration predicted from the model. The reactor model Eq. (35) were solved numerically using the program MODEST [14] during the parameter estimation and backward difference method suitable for stiff differential equations [15]. The objective function was minimized with Levenberg–Marquardt method [16]. The results from the model simulations with experimental data are presented in Figs. 3 and 5a. The figures show that the model parameters are reasonably well-identified and

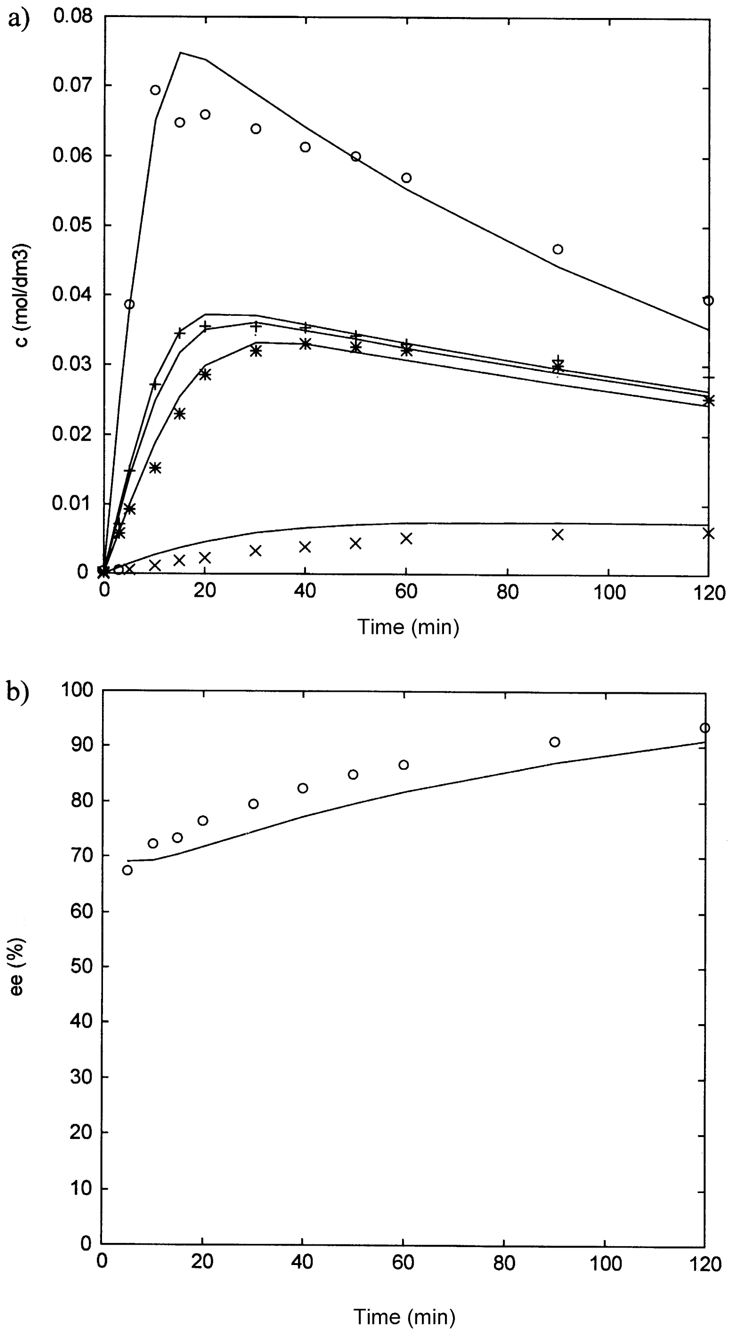

Fig. 5. (a) The yields of (*R*)-1-hydroxy-1-phenylpropanone (**B**) in the enantioselective hydrogenation of 1-phenyl-1,2-propanedione (**A**) at three different temperatures and initial concentrations of 1-phenyl-1,2-propanedione. Symbols: (○) 25°C, 0.1 mol dm^{-3}, (+) 25°C, 0.05 mol dm^{-3} and (×) 25°C, 0.01 mol dm^{-3}, (·) 15°C, 0.05 mol dm^{-3} and (∗) 0°C, 0.05 mol dm^{-3}, (b) the ee of **B** in the hydrogenation of **A** at 25°C with the initial concentration of **A** 0.1 mol dm^{-3}. The solid lines represent the model fitting.

the model is able to determine the kinetics of hydrogenation as well as the distribution of the enantiomers. Our model also predicted the trend, the increase in ee as a function of time, which was observed in kinetic experiments (Fig. 5b).

4. Conclusions

The kinetic model based on selective and unselective reaction routes in the hydrogenation of **A** was developed and tested with experimental data. Irreversible hydrogen addition was assumed to be the rate determining step and the reversible adsorption of modifier and organic compounds was assumed to be rapid. This model gave a sufficient description of the experimentally observed kinetics including both the effects of different initial concentrations of **A** and different temperatures. The observed increasing trend of the ee as a function of time was predicted correctly by our kinetic model.

Acknowledgements

The authors are grateful to Mr. Markku Reunanen for his contribution to the GC–MS analyses and to Mr. Kari Eränen for the construction of the hydrogenation equipment. The financial support received from the Academy of Finland and the Graduate School in Chemical Engineering is gratefully acknowledged.

References

[1] H.-U. Blaser, H.-P. Jalett, M. Garland, M. Studer, H. Thies, A. Wirth-Tijani, J. Catal. 174 (1998) 282.
[2] J. Wang, C. LeBlond, C. Orella, Y. Sun, J. Bradley, D. Blackmond, in: H.-U. Blaser, A. Baiker, R. Prins (Eds.), Heterogeneous Catalysis and Fine Chemicals, Vol. IV, Elsevier, Amsterdam, Stud. Surf. Sci. Catal. 108 (1997) 183.
[3] J. Margitfalvi, M. Hegedüs, E. Tfirst, Tetrahedron Asymmetry 7 (1996) 571.
[4] D. Murzin, Ind. Eng. Chem. Res. 36 (1997) 4784.
[5] E. Toukoniitty, P. Mäki-Arvela, M. Kuzma, A. Villela, A. Kalantar Neyestanaki, T. Salmi, R. Sjöholm, R. Leino, E. Laine, J. Catal. (2001), submitted for publication.
[6] E. Toukoniitty, P. Mäki-Arvela, A. Kalantar Neyestanaki, T. Salmi, A. Villela, R. Leino, R. Sjöholm, E. Laine, J. Väyrynen, T. Ollonqvist, Stud. Surf. Sci. Catal. 130 (2000) 3363.
[7] W. Adam, M. Diaz, R. Fell, C. Saha-Möller, Tetrahedron Asymmetry 7 (8) (1996) 2207.
[8] D. Gala, D. DiBenedetto, J. Clark, B. Murphy, D. Schumacher, M. Steinman, Tetrahedron Lett. 37 (5) (1996) 611.
[9] P. Wells, A. Wilkinson, Top. Catal. 5 (1998) 39.
[10] M. Studer, V. Okafor, H.-U. Blaser, J. Chem. Soc., Chem. Commun. (1998) 1053.
[11] J. Slipszenko, S. Griffiths, P. Johnston, K. Simons, W. Vermeer, P. Wells, J. Catal. 179 (1998) 267.
[12] W. Vermeer, A. Fulford, P. Johnston, P. Wells, J. Chem. Soc., Chem. Commun. (1993) 1053.
[13] P. Fogg, W. Gerrard, Solubility of Gases in Liquids, Wiley, New York, 1991, p. 307.
[14] H. Haario, MODEST — Software for Parameter Estimation, 1994, Profmath Oy, Helsinki, 1994.
[15] A. Hindmarsh, ODEPACK: a systemized collection of ODE solvers, in: Stepleman, et al. (Eds.), Scientific Computing, Vols. 55–64, IMACS, Amsterdam, 1983.
[16] D. Marquardt, An algorithm for least squares estimation on nonlinear parameters, SIAM J. 11 (1963) 431.